Electronic Supplementary Information for:

# Effect of 4-vinylpyridine incorporation on the shape transformation of poly(ethylene glycol)-*block*-polystyrene polymersomes

Işıl Yeşil Gür[a], Duru Ulukan[b], Jingxin Shao[a], Yiğitcan Sümbelli[a], Alexander B. Cook[a], Johan P.A. Heuts[c], Jan C.M. van Hest*[a], and Loai K.E.A. Abdelmohsen*[a]

[a]Bio-Organic Chemistry, Institute for Complex Molecular Systems (ICMS), Eindhoven University of Technology, 5600 MB Eindhoven, The Netherlands

[b]Department of Chemistry, Boğaziçi University, Bebek, Istanbul 34342, Turkey

[c]Supramolecular Polymer Chemistry, Department of Chemical Engineering & Chemistry, Institute for Complex Molecular Systems (ICMS), Eindhoven University of Technology, 5600 MB Eindhoven, The Netherlands

*Corresponding authors: Jan van Hest – j.c.m.v.hest@tue.nl

Loai Abdelmohsen – l.k.e.a.abdelmohsen@tue.nl

## 1. Materials and Experimental Procedures

### 1.1. Materials

Poly(ethylene glycol) methyl ether (Mn=2kDa; Sigma-Aldrich, 99%), 4-cyano-4-[(dodecylsulfanylthiocarbonyl)sulfanyl]pentanoic acid (Sigma-Aldrich, 97%) (CTA), 4-dimethylaminopyridine (Acros Organics, 99%), *N*,*N*′-dicyclohexylcarbodiimide (Sigma-Aldrich, 99%), 1,1'-azobis(cyclohexanecarbonitrile) (Sigma-Aldrich, 98%), dichloromethane (Biosolve, 99.9%), diethylether (Biosolve, 99.5%), toluene (Biosolve, 99.7%), methanol (Biosolve, 99.8%) were used as received. Styrene (Sigma-Aldrich, 99%) and 4-vinylpyridine (Sigma-Aldrich, 95%) were purified by passing through basic alumina oxide prior to use. All used solvents were analytical grade.

### 1.2. Instrumentation

*Nuclear Magnetic Resonance (NMR):* Proton nuclear magnetic resonance measurements were conducted on a Bruker 400 Ultrashield™ spectrometer, using deuterated chloroform ($CDCl_3$) as a solvent and tetramethylsilane (TMS) as internal standard.

*Gel Permeation Chromatography (GPC):* Gel permeation chromatography measurements were performed on a Shimadzu Prominence-*i* equipped with a Shimadzu RID-20A differential refractive index detector utilizing Polymer Laboratories PL gel 5 µm mixed D and mixed C

columns. THF was used as an eluent with flow rate of 1 mL/min. PS standards were used for calibration.

*Dynamic Light Scattering (DLS) and Zeta potential:* DLS and zeta potential measurements were performed on a Malvern Zetasizer Nano ZSP equipped with a 633 nm He-Ne laser. Hydrodynamic size and zeta potential of the samples was analysed at room temperature in triplicate measurements. 0.01x PBS buffer with target pH values was used for zeta potential measurements. Zetasizer software was used to process and analyse the data.

*Scanning Electron Microscopy (SEM):* Scanning electron microscopy (FEI Quanta 200 3D FEG) at a voltage of 5.00 kV was used to analyse sample morphology. 10 µL of samples (0.5-0.7 mg/mL,) were spread on a silicon wafer, air dried and coated with a gold layer via a sputter coater (Quorum Q150T plus Coater System). Image J software was used to process the data.

*Transmission Electron Microscopy (TEM)*: Transmission electron microscopy (FEI Titan Themis) at a voltage of 300 kV was used to analyse sample morphology. Carbon film coated 200 mesh copper grids were glow discharged for 40 seconds at a current of 5 mA using the Cressington 208 Carbon Coater. The 15 µL of sample solutions (0.3-0.4 mg/mL) were dropped on the grid and air dried. Image J software was used to process the data.

*Asymmetric Flow Field-Flow Fractionation (AF4):* a Wyatt Eclipse® Neon with dilution control module connected with Waters Arc™ HPLC system was used for analysis. The instrument system has four detectors; a Waters UV detector, a Wyatt Dawn® 8 multi angle light scattering detector (32°, 44°, 57°, 72°, 90°, 108°, 126°, 141°), a Wyatt QELS (90°)and a Wyatt Optilab® on-line differential refractometer. For separation, an Eclipse™ long channel with 350 µm fixed spacer equipped with a 10 kDa regenerated cellulose (RC) membrane (Neon) was used. Prior to the measurements detectors were normalized using a Bovine Serum Albumin standard. 1xPBS solvent with 0.01wt% $NaN_3$ was used as a buffer and the data processing was done using Astra 7.3.2. Sample concentrations between 3-4 mg/mL were used and 10 µL samples were injected. The applied method is given below.

| **Mode** | **Duration (min)** | **Cross flow start (mL/min)** | **Cross flow stop(mL/min)** |
|---|---|---|---|
| Elution | 2 | 1 | 1 |
| Focus | 1 | 1 | 1 |
| Focus + Inject | 3 | 1 | 1 |
| Focus | 5 | 1 | 1 |
| Elution | 5 | 1 | 1 |

| | | | |
|---|---|---|---|
| Elution | 5 | 1 | 0.2 |
| Elution | 20 | 0.2 | 0.1 |
| Elution | 20 | 0.1 | 0.1 |
| Elution | 5 | 0 | 0 |
| Elution+ Inject | 5 | 0 | 0 |
| Elution | 2 | 1 | 1 |

Channel flow 1 mL/min, Inject flow 0.2 mL/min, Detector flow 0.5 mL/min. Focusing 25%

### 1.3. Synthesis of block copolymers

Poly(ethylene glycol)-*block*-poly(styrene-*co*-4-vinyl pyridine) polymers were synthesized via reversible addition–fragmentation chain-transfer polymerization (RAFT). First, a macro-RAFT agent was synthesized by esterification of monomethoxy PEG with a chain-transfer agent (CTA). Poly(ethylene glycol) methyl ether (2.0 g, 1.0 mmol) and 4-cyano-4-[(dodecylsulfanylthiocarbonyl)sulfanyl]pentanoic acid (600.0 mg, 1.49 mmol) were dissolved in 10 mL of dry dichloromethane (DCM) and stirred in an ice bath under argon. In a separate vial, N,N′-dicyclohexylcarbodiimide (DCC, 310.8 mg, 1.51 mmol) and 4-(dimethylamino)pyridine (DMAP, 19.2 mg, 0.16 mmol) were dissolved in dry DCM and kept under argon. This solution was added dropwise to the PEG solution while stirring in the ice bath. The reaction mixture was kept stirring under cold conditions and argon for an additional 30 minutes, after which the reaction was allowed to proceed at room temperature for three days. A white precipitate formed, which was filtered off, and the final product was purified by precipitation in cold diethyl ether (DEE) and obtained by drying in vacuum oven (1.7 g, 0.7 mmol, 72%).

$^1$H NMR (400 MHz, $CDCl_3$) δ = 4.25 (t, 2H), 3.81 (t, 2H), 3.67 – 3.56 (m, 176H), 3.37 (s, 3H), 3.32 (t, 2H), 2.65 (t, 2H), 2.59 – 2.46 (m, 1H), 2.43 – 2.31 (m, 1H), 1.87 (s, 3H), 1.72 – 1.65 (m, 2H), 1.43 – 1.35 (m, 2H), 1.31 – 1.21 (m, 16H), 0.88 (t, 3H).

Different amphiphilic block copolymers were synthesized by varying the feed ratios of styrene (St) and 4-vinylpyridine (4VP). Three block copolymers (A-(B-C)/x) were prepared by adding St and 4VP together at the beginning of polymerization. The other two block copolymers (A-B-C and A-C-B) were synthesized by sequential addition: one monomer was polymerized to completion before adding the second monomer. As an example, the RAFT polymerization of PEG-*b*-P($S_{160}$-*co*-$4VP_{10}$) was carried out as follows: poly(ethylene glycol) methyl ether (4-cyano-4-pentanoate dodecyl trithiocarbonate) ($mPEG_{44}$-CTA) (105.90 mg, 0.04 mmol), styrene (910 mg, 8.74 mmol), 4-vinylpyridine (45.83 mg, 0.44 mmol), and 100 µL of 0.021 mg/µL 1,1′-azobis(cyclohexanecarbonitrile) (ACHC) initiator solution in toluene were added to a

reaction vessel and stirred under argon. The flask was then placed in a preheated oil bath at 90 °C, and the reaction was allowed to proceed for one day. After termination, the reaction mixture was dissolved in chloroform and precipitated into cold methanol. The resulting white–yellowish precipitate was collected and analysed by NMR and GPC.

$^1$H NMR (400 MHz, $CDCl_3$) δ = 8.22 (s, 20H), 7.08 (m, 475H), 6.52 (m, 336H), 3.65 (s, 176H), 3.38 (s, 3H), 1.84 (m, 192H), 1.43 (m, 397H).

Detailed synthesis conditions and characterization data for all polymers are summarized in Table S1.

Table S1. RAFT polymerization details

| | **$[M_{St}]/[CTA]$** | **$[M_{4VP}]/[CTA]$** | **$[CTA]/[I]$** | **$M_n$[a] (kg mol$^{-1}$)** | **Đ[b]** |
|---|---|---|---|---|---|
| **P1: A-(B-C) / 0.06** PEG-*b*-P(S160-*co*-4VP10) | 198 | 10 | 5 | 20 | 1.09 |
| **P2: A-(B-C) / 0.11** PEG-*b*-P(S155-*co*-4VP20) | 198 | 20 | 5 | 21 | 1.07 |
| **P3: A-(B-C) / 0.14** PEG-*b*-P(S190-*co*-4VP30) | 230 | 30 | 5 | 26 | 1.11 |
| **P4: A-B-C / 0.06** PEG-*b*-PS150-*b*-P4VP10 | 199 | 10 | 5 | 19 | 1.09 |
| **P5: A-C-B / 0.09** PEG-*b*-P4VP15-*b*-PS150 | 200 | 10 | 5 | 20 | 1.10 |

[a]Number average molecular weight was calculated from $^1$H-NMR measurements. [b]Polydispersity measured by gel permeation chromatography (GPC). Polymers are denoted as A-(B-C)/x, where x represents the mole fraction of 4VP within the hydrophobic block.

Kinetic studies were performed to determine the copolymerization rates of styrene and 4-VP. Seven polymerizations were executed varying the 4VP content from 10% to 90%. These reactions were stopped below 10% conversion, and the samples were analysed by $^1$H NMR spectroscopy (Figure S8 and S9). Based on the monomer integral peaks, both the Fineman–Ross and Kelen–Tüdös methods were used to calculate the reactivity ratios (Figure S10). The Fineman–Ross method yielded reactivity ratios of $r_{4VP} = 0.50$ and $r_{St} = 1.19$, while the Kelen–Tüdös method gave $r_{4VP} = 0.51$ and $r_{St} = 1.23$.

Previous studies on the free radical polymerization of styrene and 4-vinylpyridine reported $r_{4VP}$ = 0.85 and $r_{St}$ = 0.41 (Fineman–Ross) and $r_{4VP}$ = 0.73 and $r_{St}$ = 0.37 (Kelen–Tüdös).[1] Another study focusing on controlled radical polymerization with TEMPO found $r_{4VP}$ = 0.96 and $r_{St}$ = 0.58 according to the Kelen–Tüdös method.[2] These values vary across the literature, making direct comparison difficult due to differences in polymerization conditions. Moreover, it has been shown that 4VP polymerization is strongly influenced by the solvent.[3]

Therefore, to determine the final polymer composition, we evaluated the instantaneous copolymer composition as a function of monomer conversion, following a recent approach in the literature.[4] As shown in Figure S11, no significant compositional drift was observed in the synthesized copolymers with the lowest 4VP content ($f_{A,0}$ = 0.06 for P1) and the highest content ($f_{A,0}$ = 0.14 for P3). This analysis indicates that the P4VP fraction remained stable throughout the reaction, with only a minor drift observed toward the end, confirming that statistical copolymers were obtained when the two monomers were added simultaneously at the beginning of the polymerization.

### 1.4. General procedure for polymer self-assembly and shape transformation

Self-assembly was carried out using the solvent-switch method. A total of 20 mg of solid polymer was dissolved in 2 mL of a THF-dioxane mixture (4:1 v/v, 10 mg/mL). Subsequently, 2 mL of Milli-Q water was added using a syringe pump at a rate of 1 mL/h. Afterwards, the organic solvent was removed by dialysis against distilled water or aqueous NaCl solutions of varying concentrations.

### 1.5. Copper coordination and CuAAC reaction

The copper nanoreactors were prepared by mixing the stomatocyte solution with $CuSO_4$ and ascorbic acid. After 2.5h incubation at 37 °C, excess copper was removed by a couple of washing cycles. In order to check activity, a model reaction was chosen between 3-azido-7-hydroxycoumarin and propargyl alcohol to have a fluorescent final product (Figure 4) which was detected by a plate reader (λex 340nm, λem 470nm). As shown in Figure 4, the copper nanoreactor catalysed the reaction and fluorescent intensity increased which indicates product formation whereas empty stomatocytes (without copper) and only the reactants themselves did not designate product formation.

## 2. Supplementary Figures

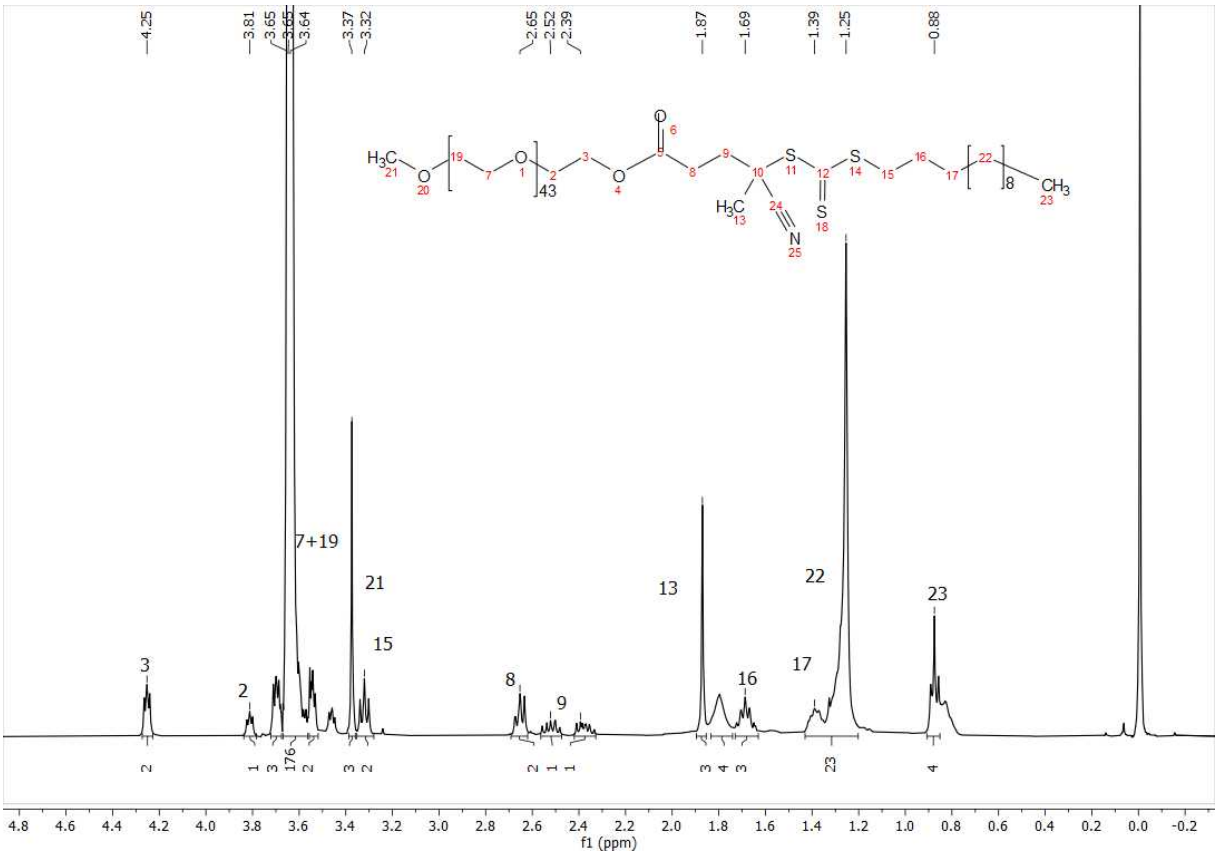


*Supplementary Figure 1. $^{1}H$ NMR spectrum of PEG-CTA.*

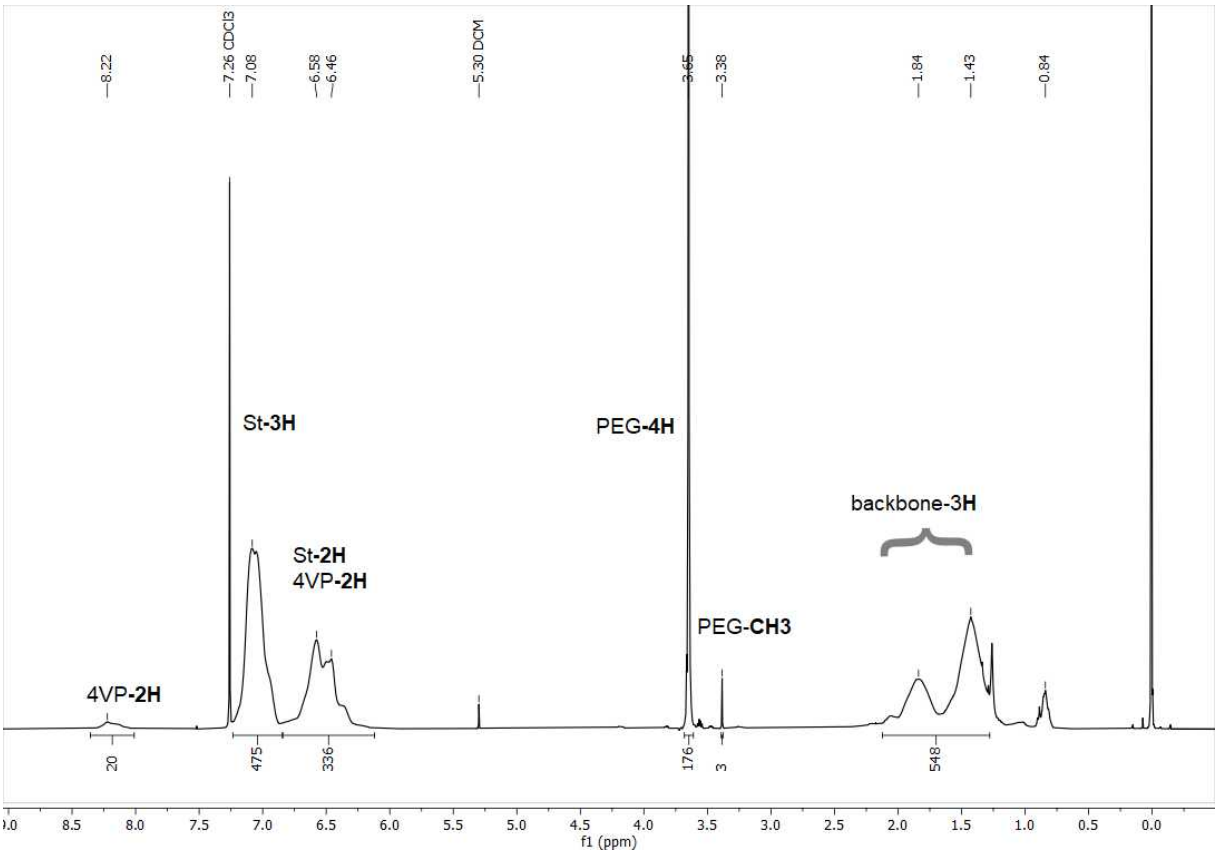


*Supplementary Figure 2. $^{1}H$ NMR spectrum of polymer $PEG_{44}$-b-$P(S_{160}$-co-$4VP_{10})$.*

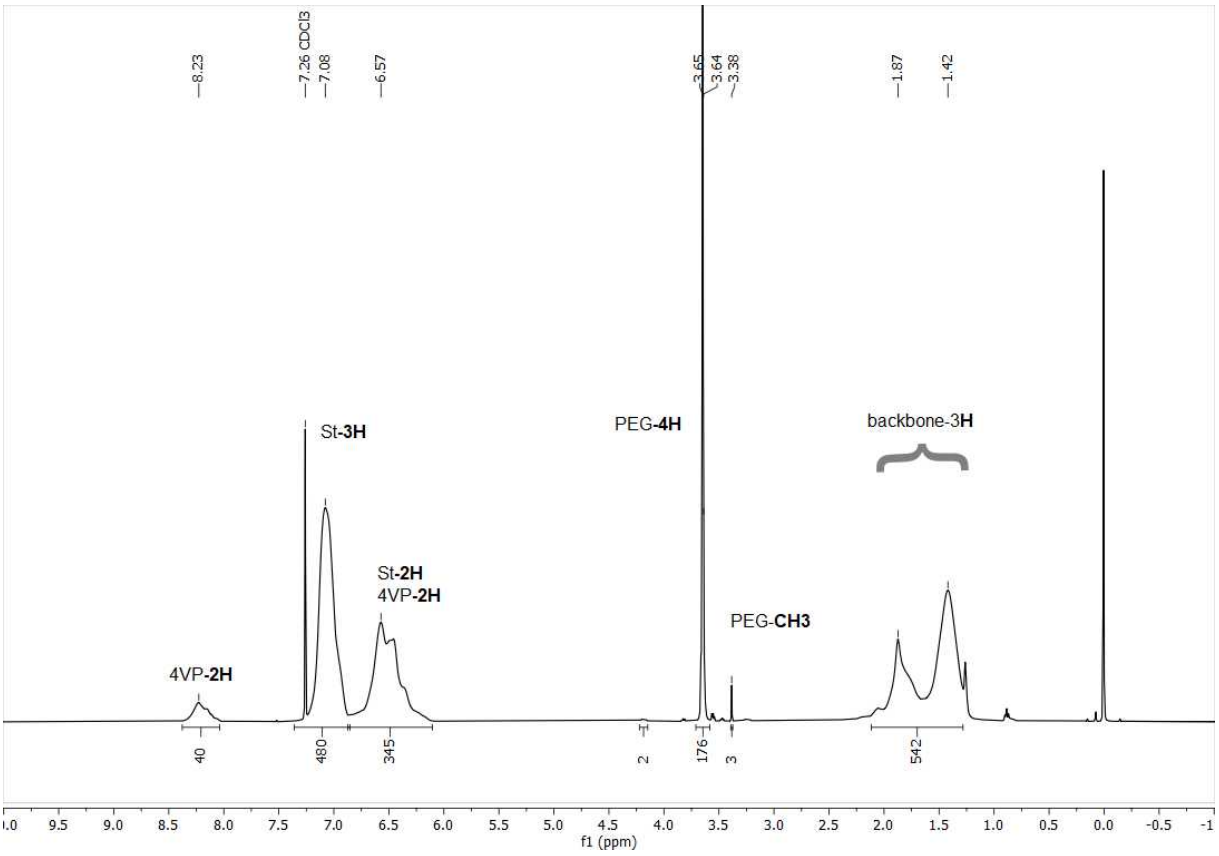


*Supplementary Figure 3.[1]H NMR spectrum of $PEG_{44}$-b-$P(S_{155}$-co-$4VP_{20})$.*

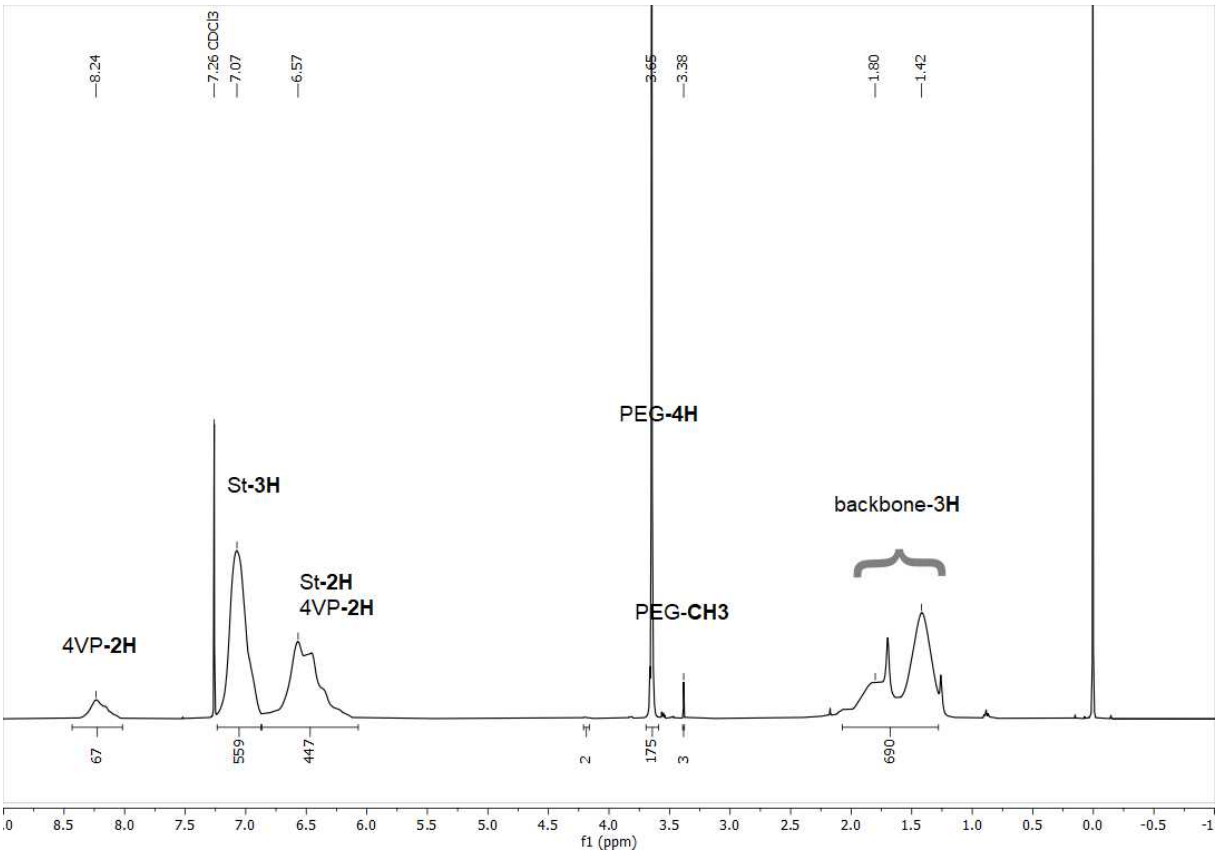


*Supplementary Figure 4. $^{1}H$ NMR spectrum of $PEG_{44}$-b-$P(S_{190}$-co-$4VP_{30})$.*

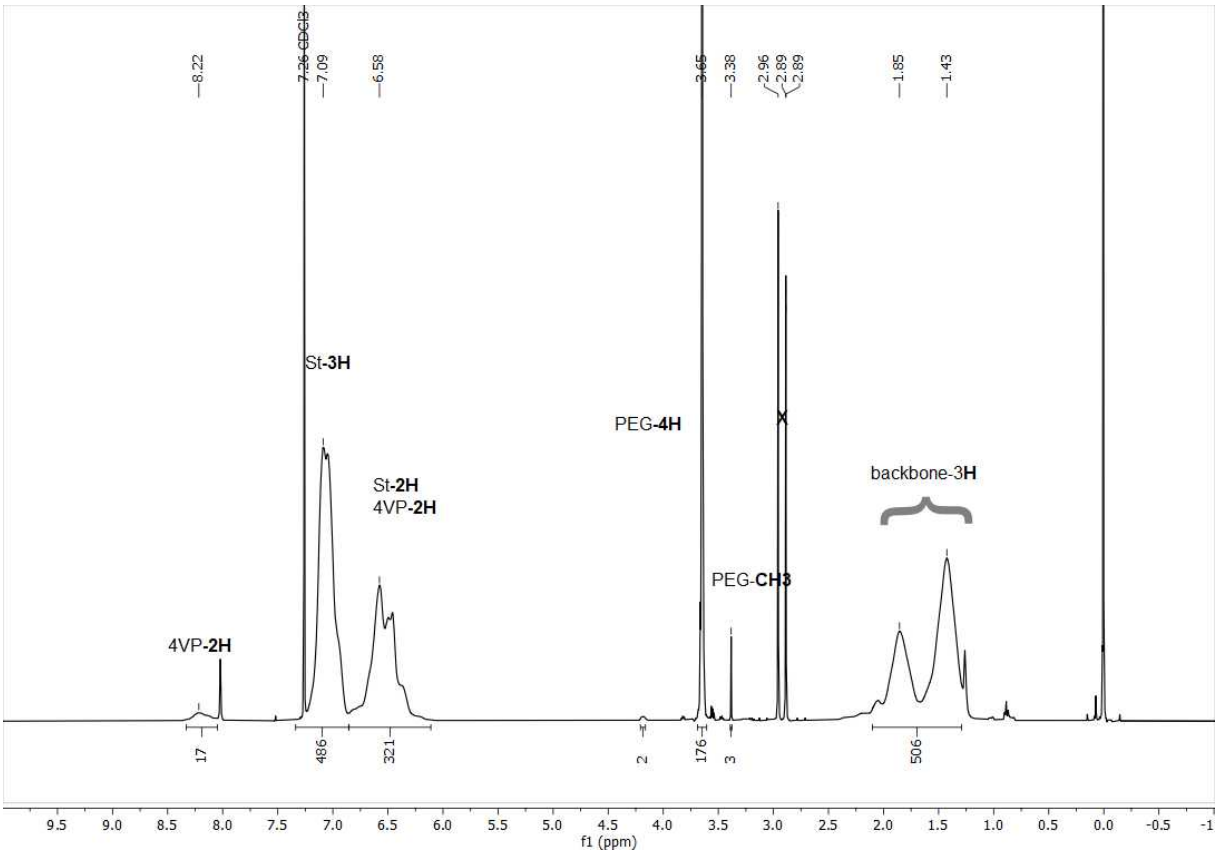


*Supplementary Figure 5. $^{1}H$ NMR spectrum of $PEG_{44}$-b-$PS_{150}$-b-$P4VP_{10}$.*

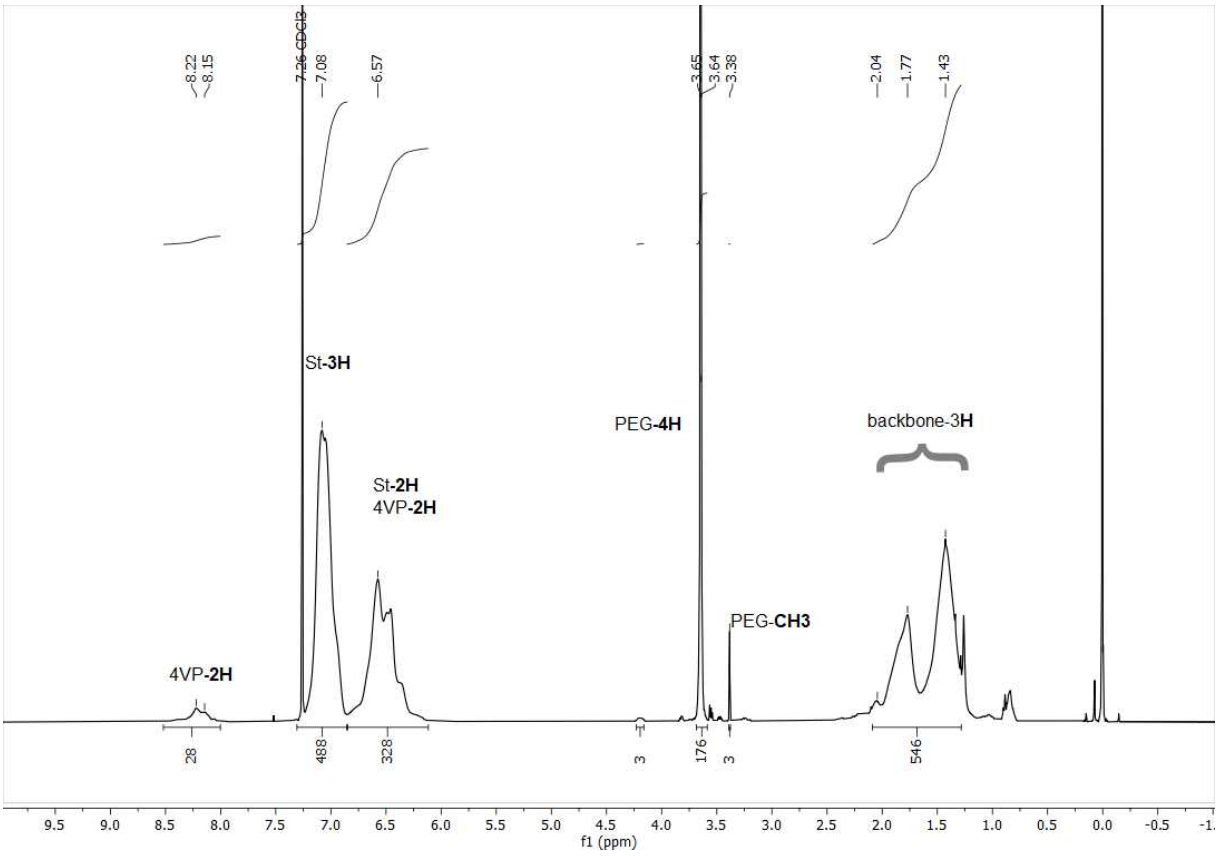


*Supplementary Figure 6. [1]H NMR spectrum of $PEG_{44}$-b-$P4VP_{15}$-b-$PS_{150}$.*

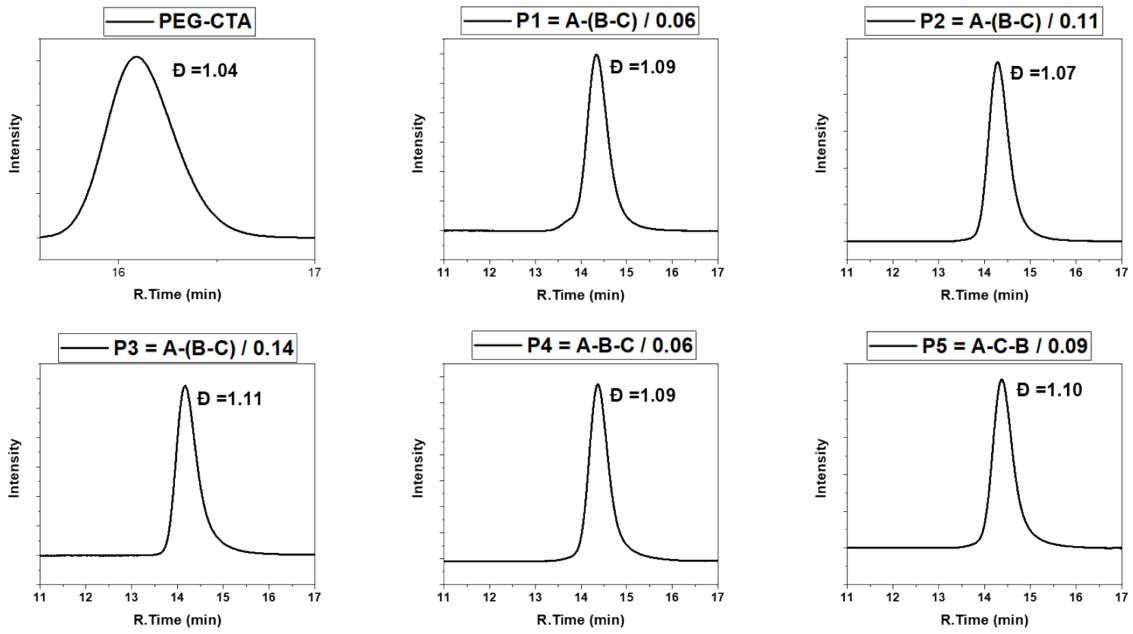


*Supplementary Figure 7. GPC chromatograms of the synthesized PEG-CTA and the block copolymers.*

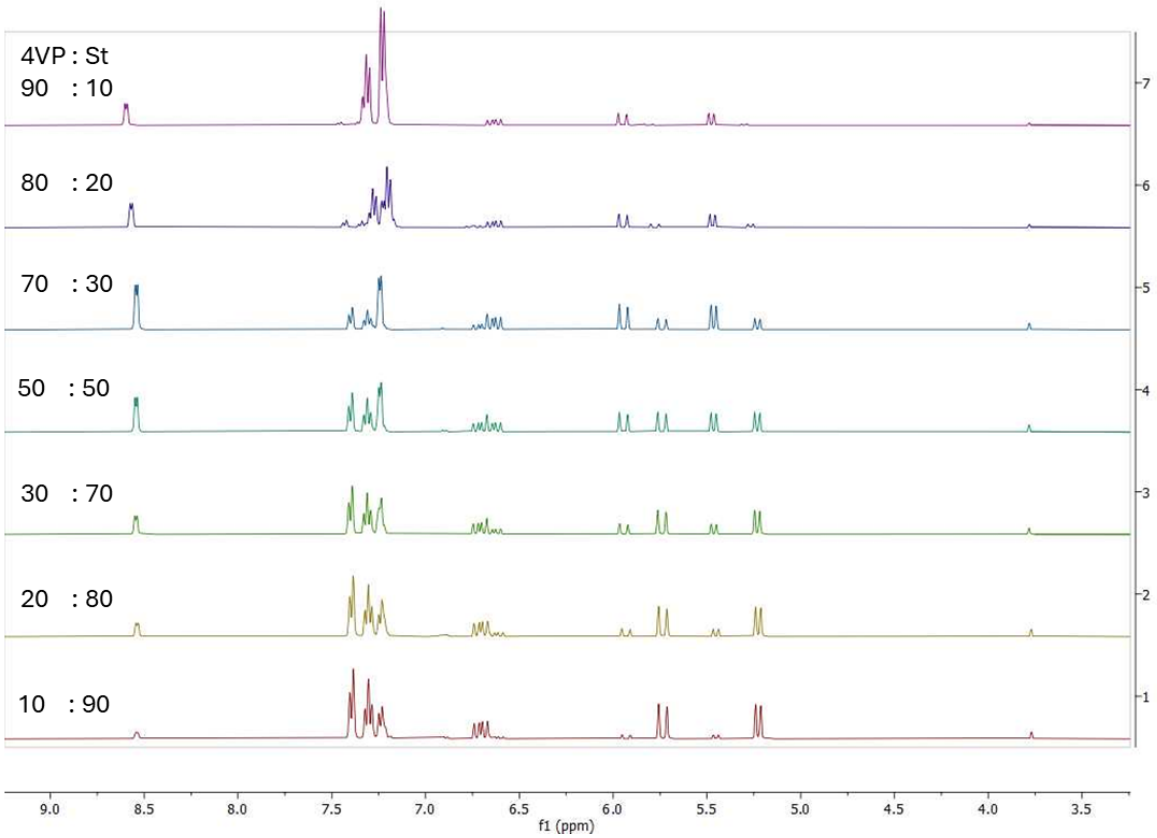


*Supplementary Figure 8. $^{1}H$ NMR spectra of seven polymerizations used for reactivity ratio calculation at t=0. The corresponding monomer feed ratios are depicted for each reaction.*

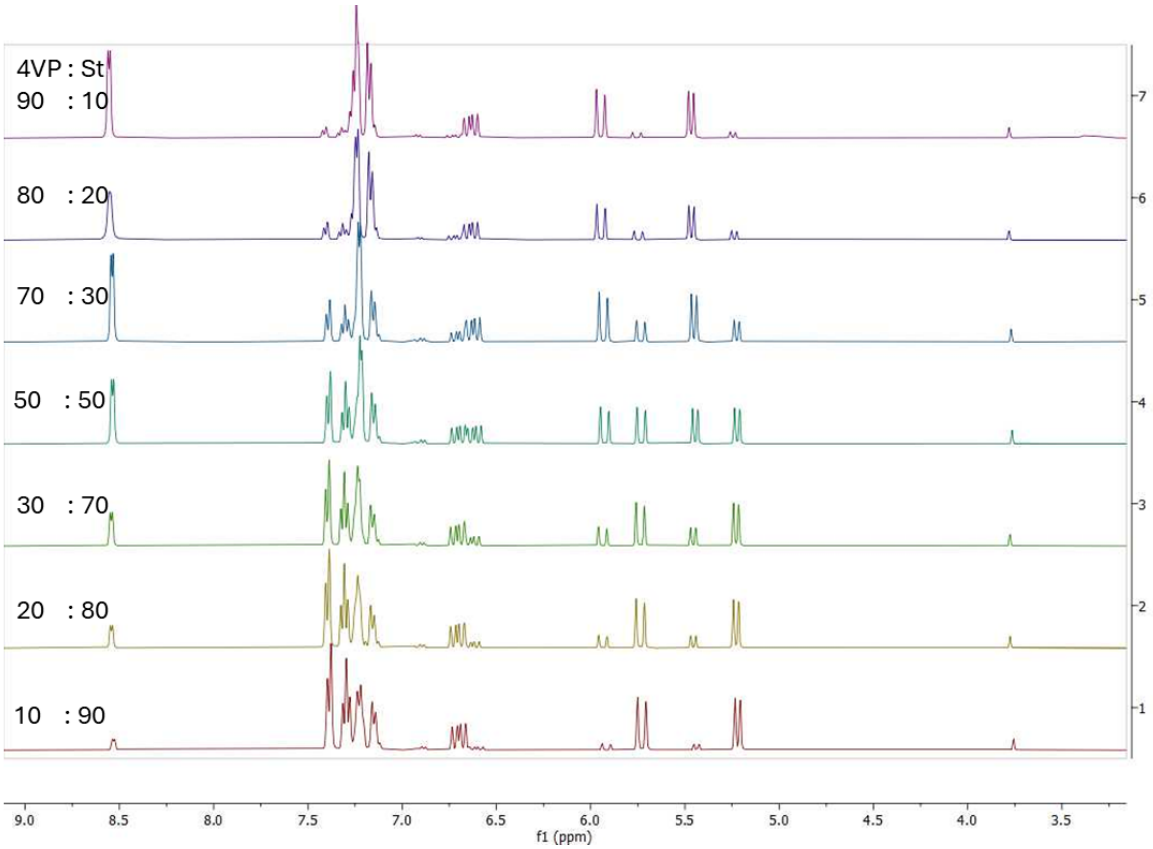


*Supplementary Figure 9. [1]H NMR spectra of seven polymerizations used for reactivity ratio calculation at t=final (15 min-45 min). The corresponding monomer feed ratios are depicted for each reaction.*

*Table S2. Parameters determined from [1]H NMR measurements used for monomer reactivity ratios.*

| $f_A$ (4VP) | $f_B$ (S) | $F_A$ (4VP) | $F_B$ (S) |
|---|---|---|---|
| 0.10 | 0.90 | 0.09 | 0.91 |
| 0.20 | 0.80 | 0.15 | 0.85 |
| 0.30 | 0.70 | 0.22 | 0.78 |
| 0.49 | 0.51 | 0.40 | 0.60 |
| 0.69 | 0.31 | 0.56 | 0.44 |
| 0.78 | 0.22 | 0.71 | 0.29 |
| 0.88 | 0.12 | 0.80 | 0.20 |

*$f_A$(4VP) and $f_B$(S) are feed ratios of the two monomers. $F_A$(4VP) and $F_B$(S) are the mole fractions of corresponding monomer in the formed polymer at t=final.

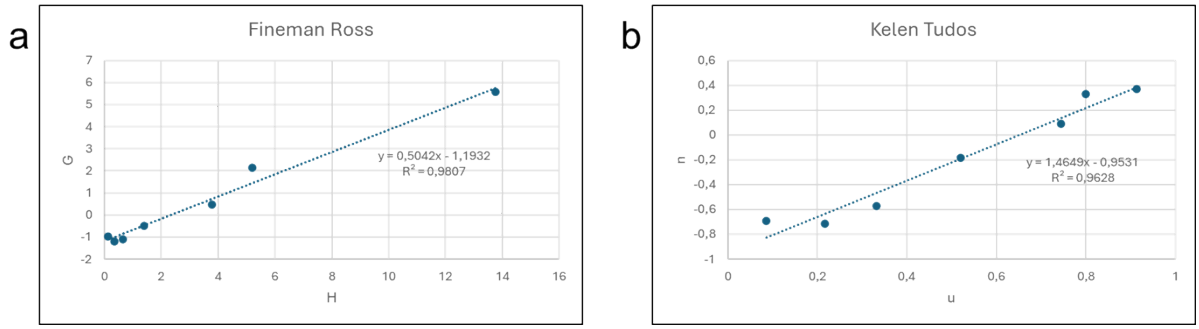


*Supplementary Figure 10. Monomer reactivity ratios determined via a) Fineman Ross method, b) Kelen Tudos method.*

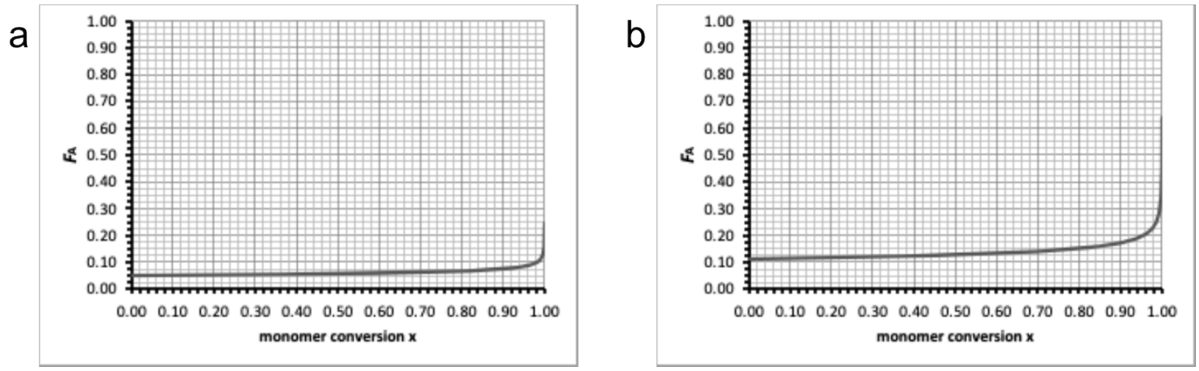


*Supplementary Figure 11. Instantaneous copolymer composition as a function of overall monomer conversion, a) $f_{A,0}$ = 0.06 (lowest ratio within synthesized polymers) and b) ) $f_{A,0}$ = 0.14 (highest ratio within the synthesized polymers); $r_{4VP}(A)$=0.5 and $r_{St}(B)$=1.2 are used.*

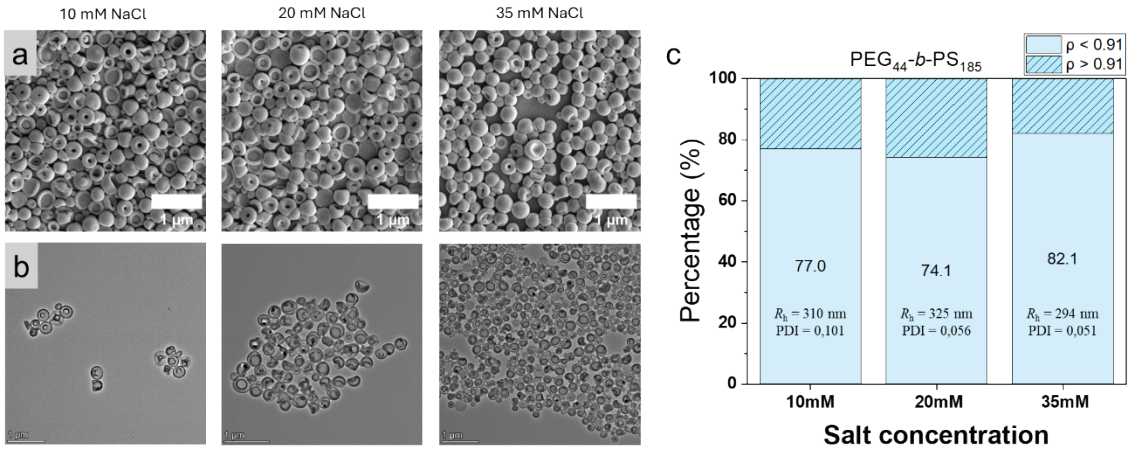


*Supplementary Figure 12. a) SEM and b) TEM images of polymersomes and stomatocytes prepared from $PEG_{44}$-b-$PS_{185}$, dialyzed against 10 mM NaCl, 20 mM NaCl and 35 mM NaCl solutions. c) Distribution analysis of polymeric vesicles calculated from light scattering*

*analysis, displaying the percentage of the stomatocytes , hydrodynamic diameter and PDI. SEM and TEM scale bar = 1 μm.*

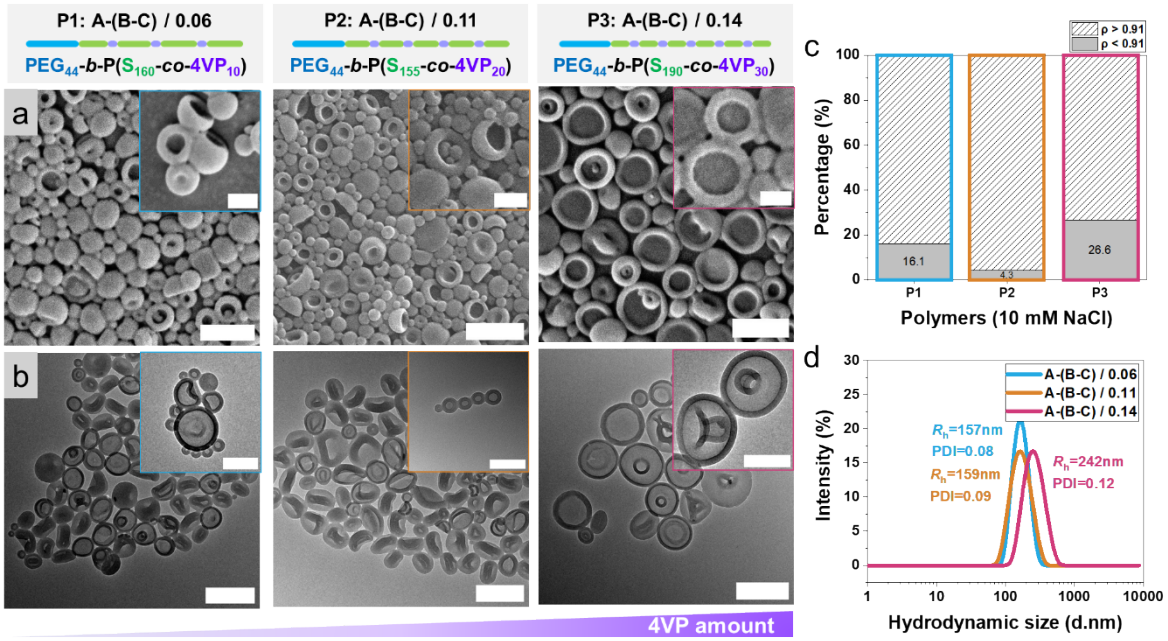


*Supplementary Figure 13. The effect of 4VP content in statistical block copolymers on polymersome formation and shape transformation upon dialysis against 10 mM NaCl. a) SEM and b) TEM images of the samples. c) Distribution analysis of polymeric vesicles calculated from light scattering analysis, displaying the percentage of the stomatocytes. d) Dynamic light scattering size intensity comparison, displaying hydrodynamic diameter and PDI. EM scale bar = 500 nm, insert scale bar = 200 nm*

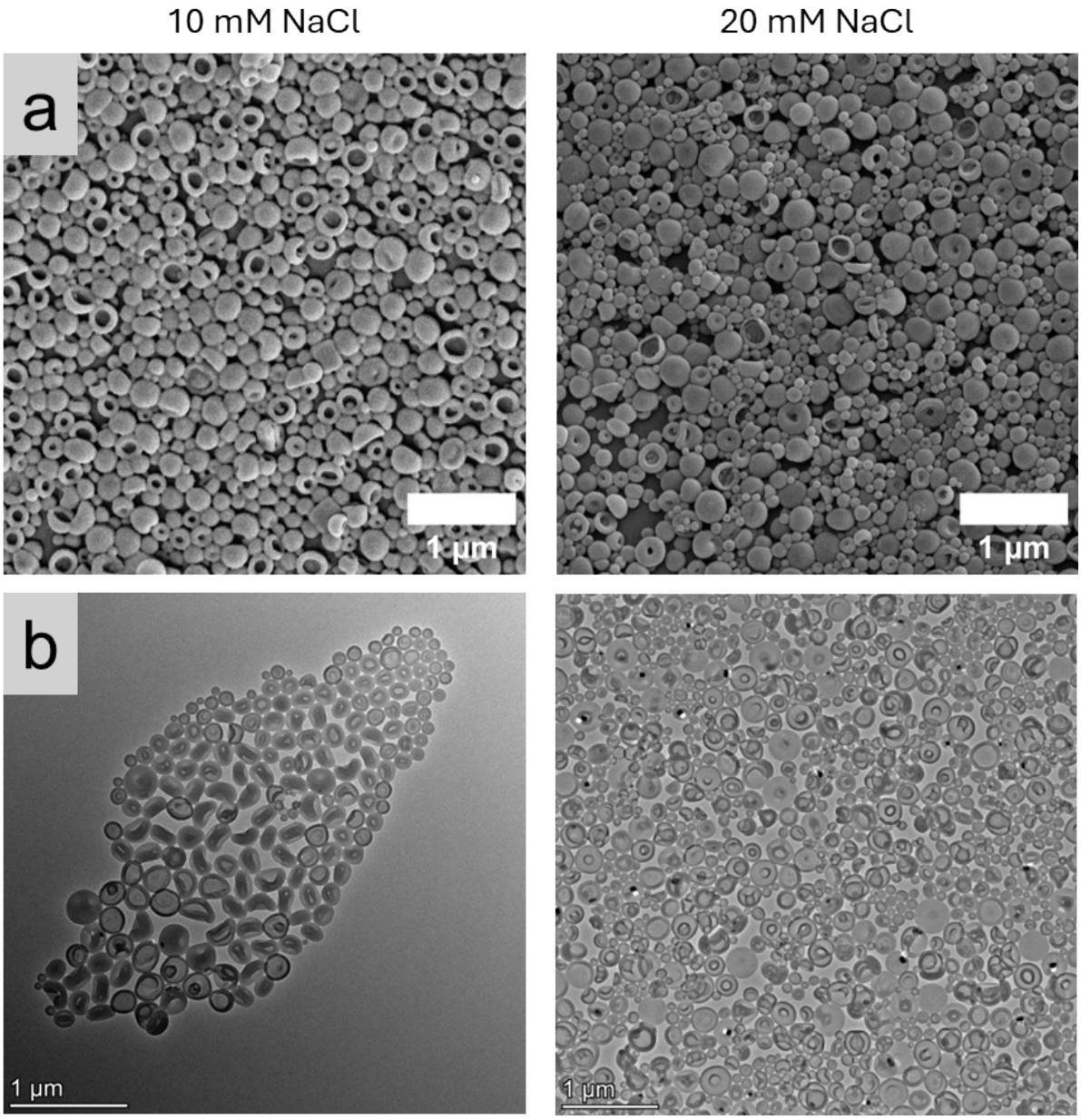


*Supplementary Figure 14. a) SEM and b) TEM images of polymer vesicles prepared from P1 = $PEG_{44}$-b-$P(S_{160}$-co-$4VP_{10})$. SEM and TEM scale bar = 1 µm.*

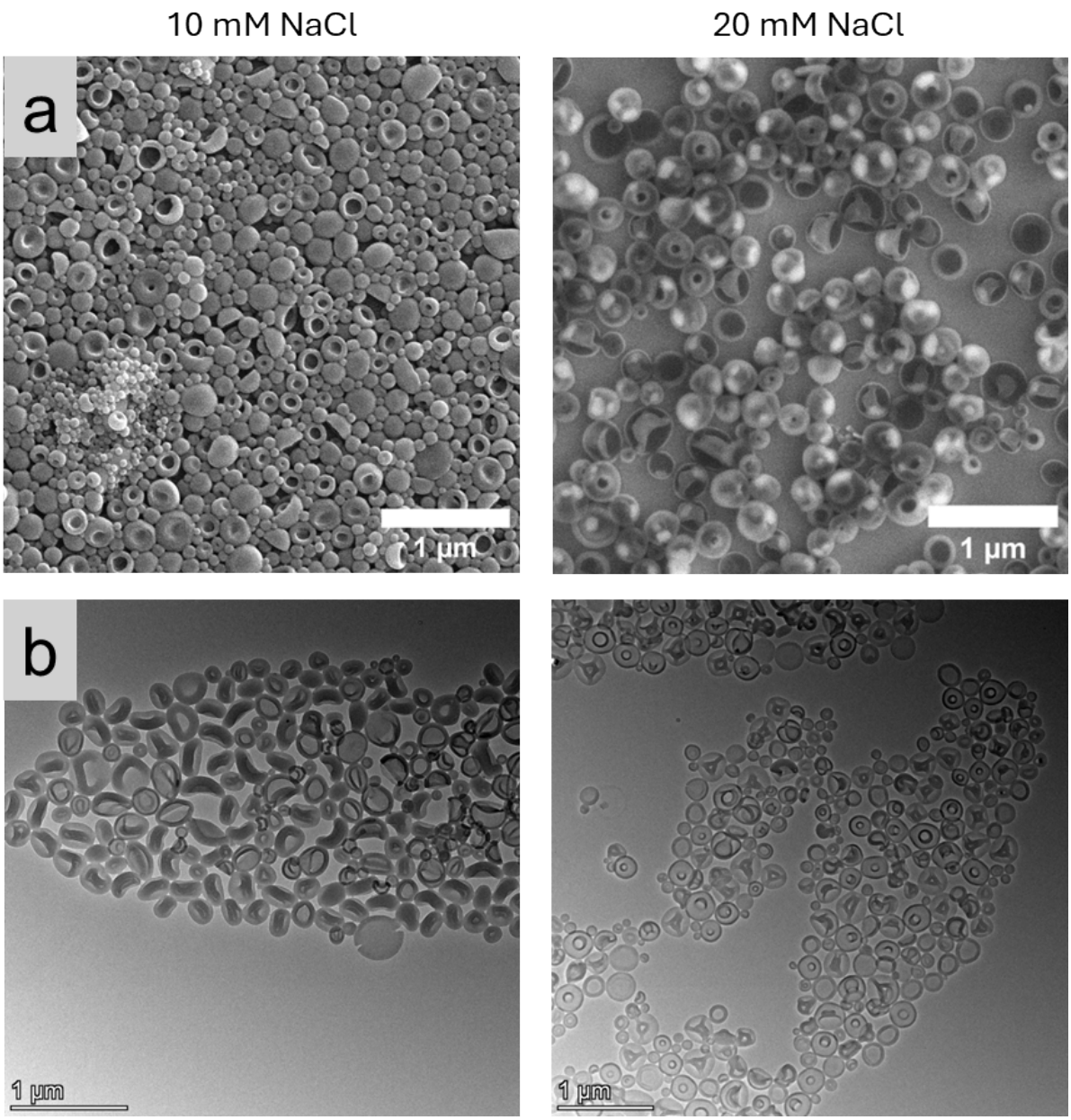


*Supplementary Figure 15. a) SEM and b) TEM images of polymer vesicles prepared from P2 = $PEG_{44}$-b-$P(S_{155}$-co-$4VP_{20})$. SEM and TEM scale bar = 1 µm*

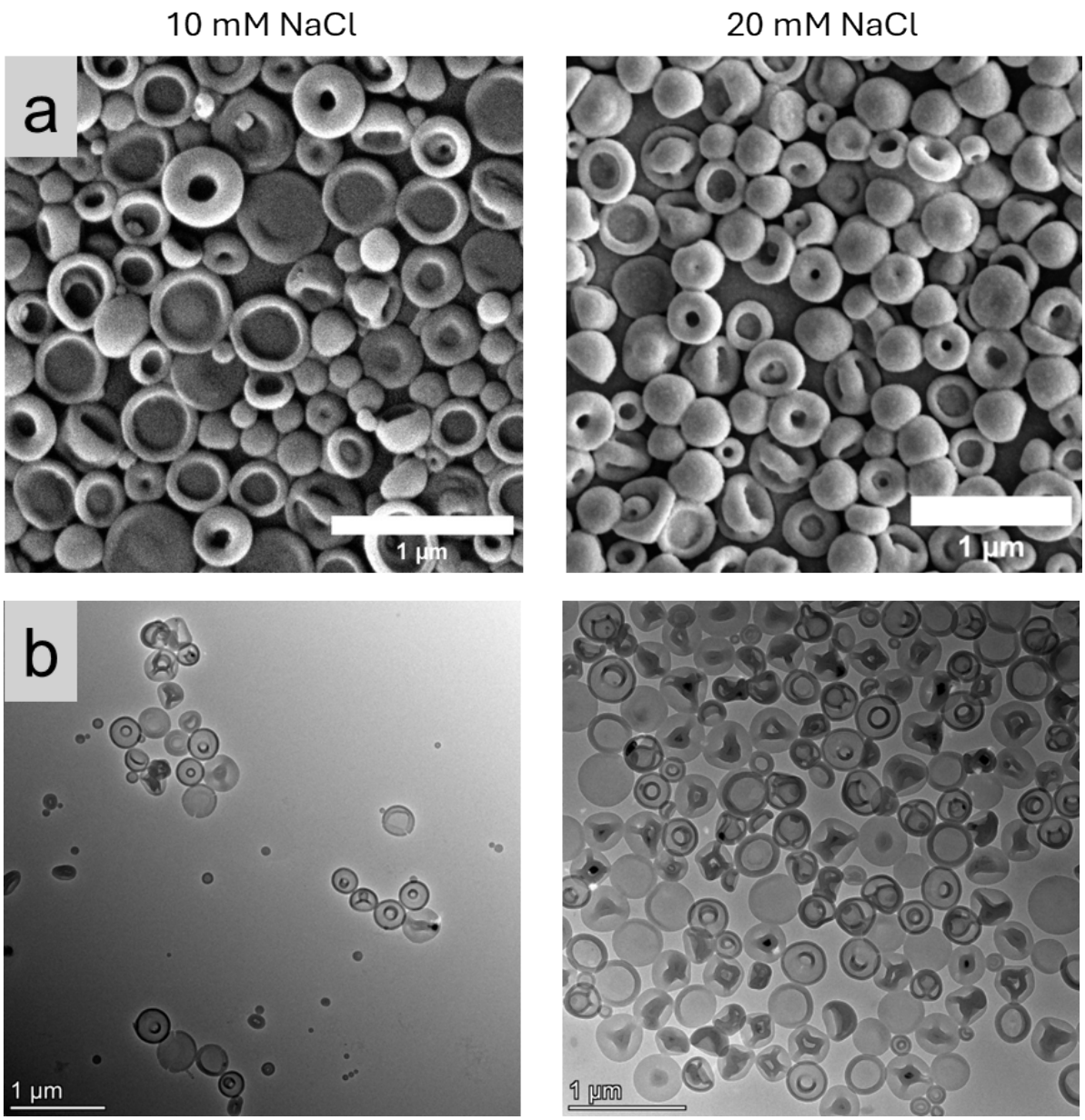


*Supplementary Figure 16. a) SEM and b) TEM images of polymer vesicles prepared from P3 = $PEG_{44}$-b-$P(S_{190}$-co-$4VP_{30})$. SEM and TEM scale bar = 1 µm.*

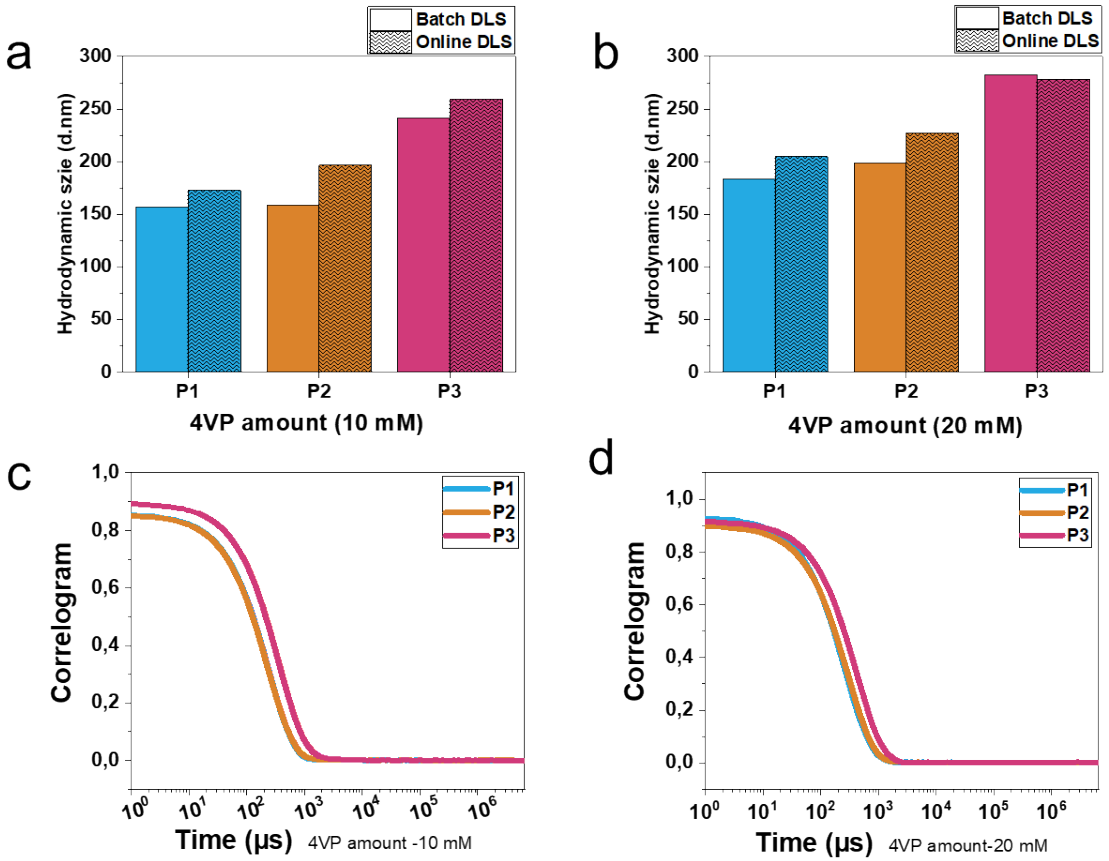


*Supplementary Figure 17. Hydrodynamic size comparison measured by batch DLS and online DLS a) for samples prepared by dialysis against10 mM NaCl, b) for samples prepared by dialysis against 20 mM NaCl. c) Batch DLS correlogram for samples prepared by dialysis against 10 mM NaCl. d) Batch DLS correlogram for samples prepared by dialysis against 20 mM NaCl. P1, P2 and P3 were used.*

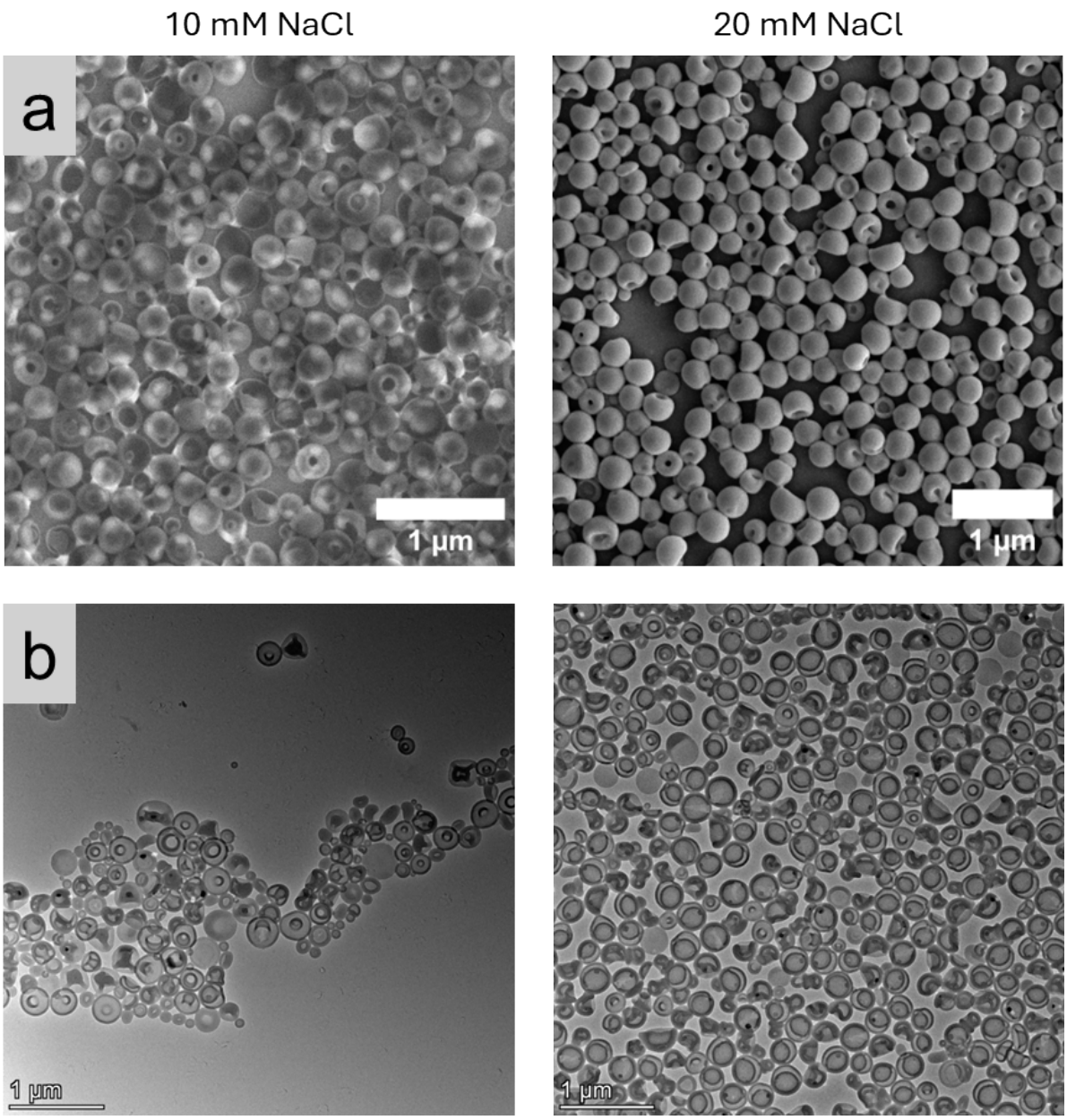


*Supplementary Figure 18. a) SEM and b) TEM images of polymer vesicles prepared from P4 = $PEG_{44}$-b-$PS_{150}$-b-$P4VP_{10}$. SEM and TEM scale bar = 1 µm.*

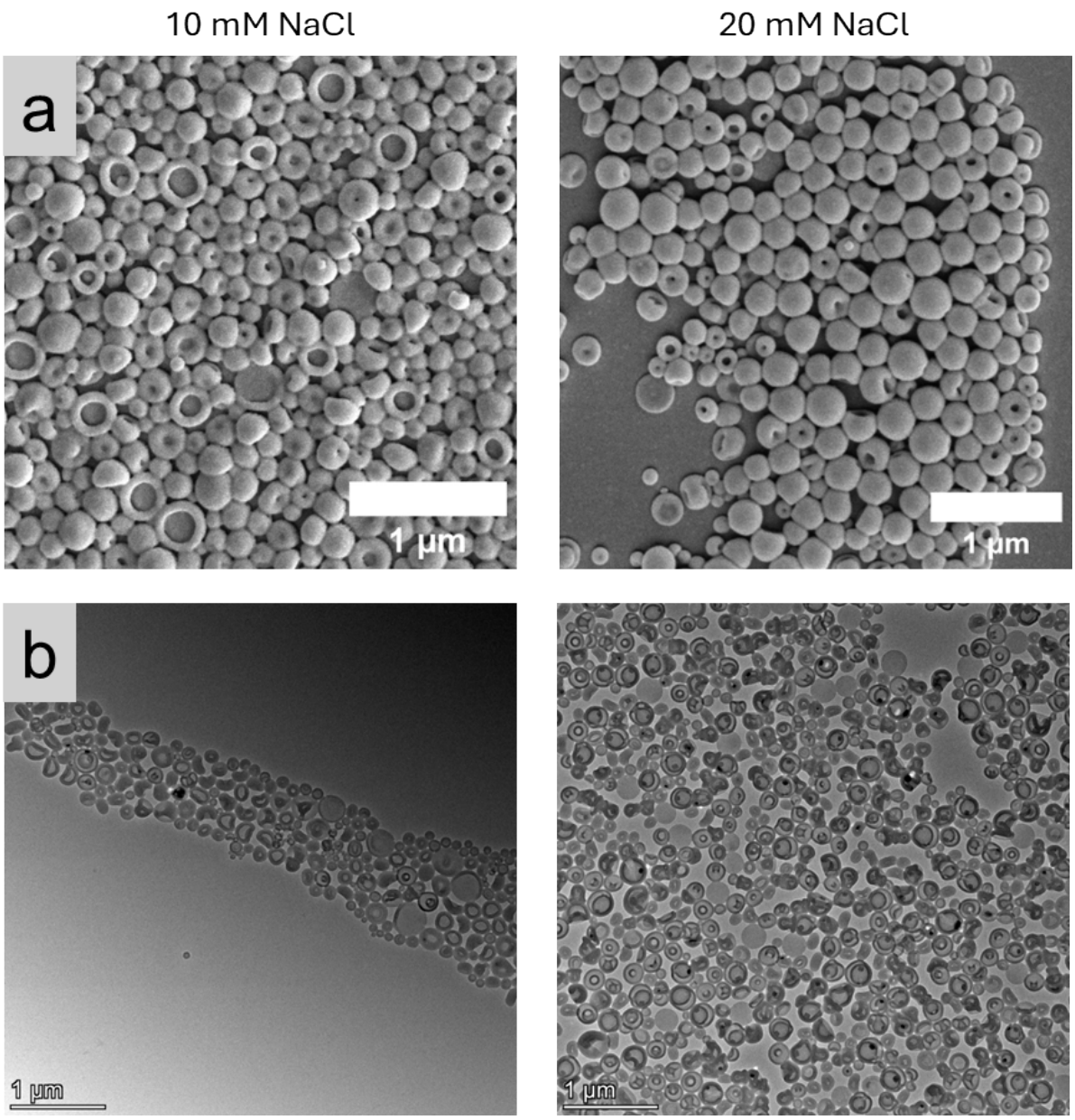


*Supplementary Figure 19. a) SEM and b) TEM images of polymer vesicles prepared from P5 = $PEG_{44}$-b-$P4VP_{15}$-b-$PS_{150}$. SEM and TEM scale bar = 1 µm.*

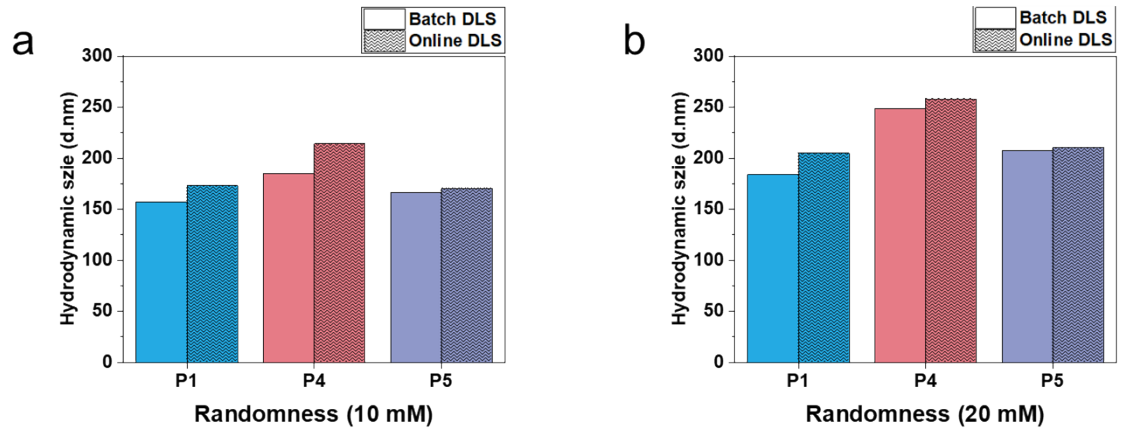


*Supplementary Figure 20. Hydrodynamic size comparison measured by batch DLS and online DLS a) for samples prepared by dialysis against 10 mM NaCl, b) for samples prepared by dialysis against 20 mM NaCl. P1, P4 and P5 were used.*

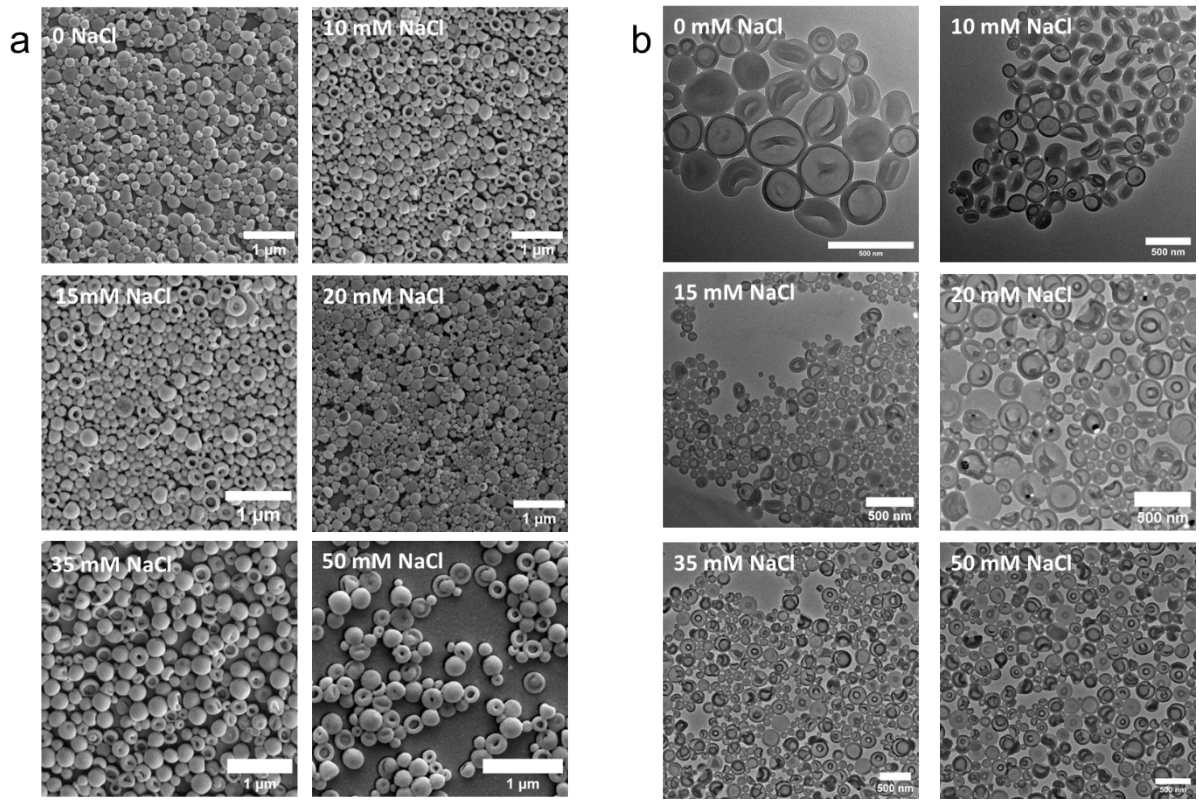


*Supplementary Figure 21. a) SEM and b) TEM images of samples prepared by dialysis against different NaCl concentrations. P1 = $PEG_{44}$-b-$P(S_{160}$-co-$4VP_{10})$ was used. SEM scale bar = 1 µm, TEM scale bar = 500 nm.*

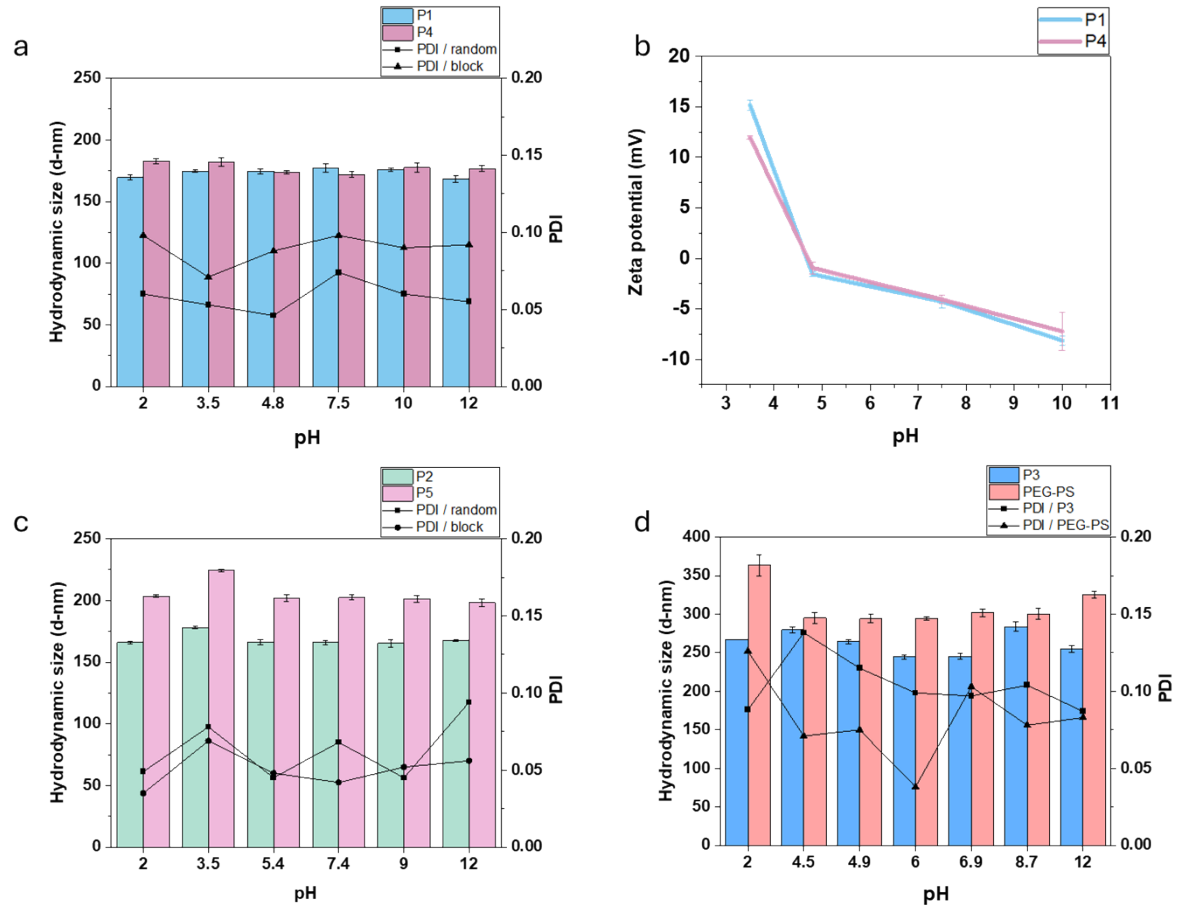


*Supplementary Figure 22. The analysis of pH effect on size. Comparison of size a) and zeta potential b) of the vesicles formed from block copolymers which have statistical and block-like architectures, containing 10 repeating units of 4VP; P1 vs P4. Comparison of the size vesicles prepared from c) P2: $PEG_{44}$-b-$P(S_{155}$-co-$4VP_{20})$ vs P5: $PEG_{44}$-b-$P4VP_{15}$-b-$PS_{150}$ and d) P3: $PEG_{44}$-b-$P(S_{190}$-co-$4VP_{30})$ vs control: $PEG_{44}$-b-$PS_{190}$.*

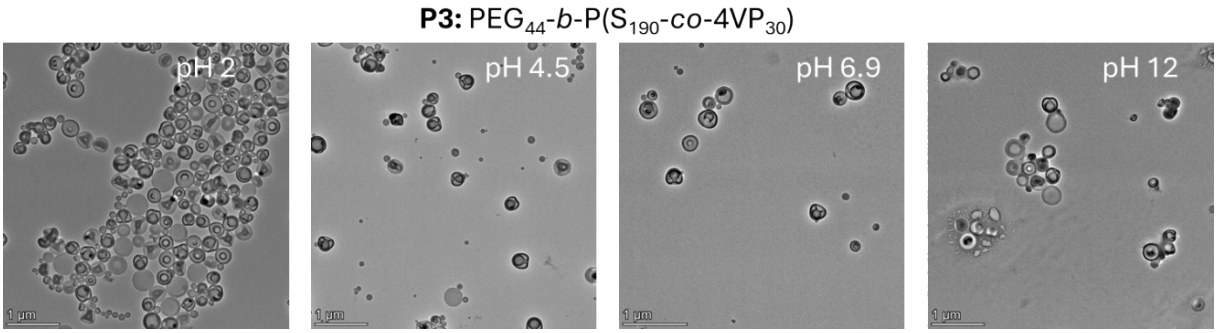


*Supplementary Figure 23. TEM images of the vesicles prepared from P3: $PEG_{44}$-b-$P(S_{190}$-co-$4VP_{30})$ in pH 2, pH 4.5, pH 6.9, and pH 12. TEM scale bar = 1 µm.*

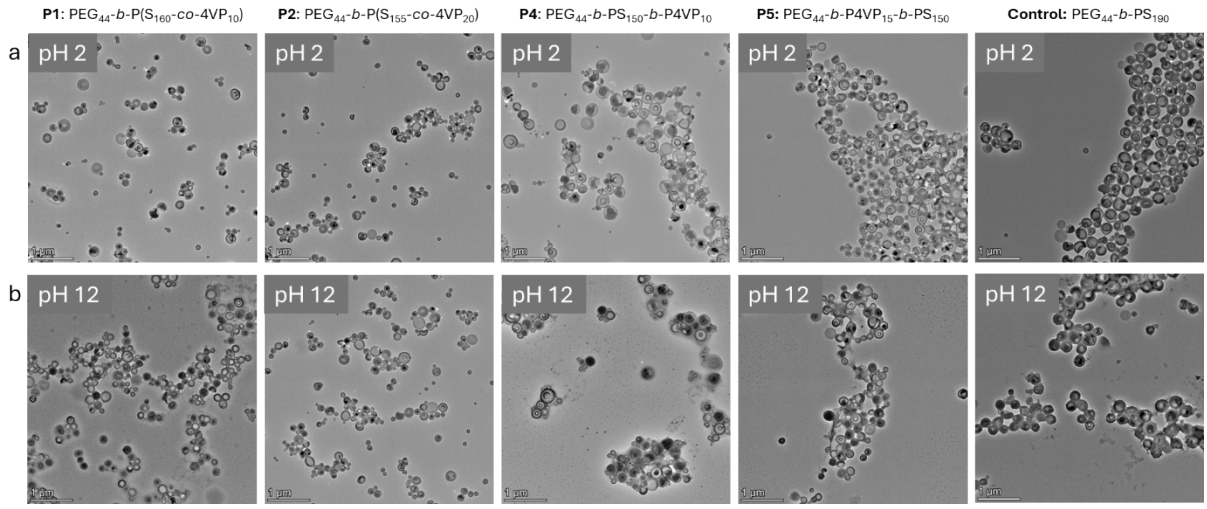


*Supplementary Figure 24. TEM images of the vesicles prepared from P1, P2, P4, P5 and control PEG-PS a) in pH 2, and b) in pH 12. TEM scale bar = 1 µm.*

## 3. References

1. E. Yilmaz and Z. Küçükyavuz, *Polymer*, 1993, **34**, 145–149.
2. M. Baumann and G. Schmidt-Naake, *Macromol. Chem. Phys.*, 2000, **201**, 2751–2755.
3. X. Zhou, W. Wang, H. Yu, J. Zhao, Z. Zhang and X. Zhu, *Polym. Chem.*, 2013, **4**, 3575.
4. J. P. A. Heuts and B. Klumperman, *European Polymer Journal*, 2024, **215**, 113215.